International Research Journal of Engineering and Technology (IRJET) e-ISSN: 2395-0056
Volume: 09 Issue: 05 | May 2022 www.irjet.net p-ISSN: 2395-0072

Critical Investigation of Influence of Al/Cr Ratio on the Properties of High Entropy Alloys

Murtaza Maajid[1], Abhishek Thakur[2]

[1]M.Tech Scholar, Universal Institute of Engineering & Technology, Lalru
[2]Assitant Professor, Universal Institute of Engineering & Technology, Lalru

---

Abstract: Due to the obvious high concentration of each superior elements, HEAs have unusual physical, chemical, mechanical, and electrochemical characteristics. HEAs also have a unique structure. In order to improve the qualities even further, certain trace amounts of elements (at. percent 5 percent) are also included. In the current investigation, the synthesis and characterisation of high-entropy alloys based on AlCoCrFeMnNi will be the primary focuses. In this study, the influence of the Al/Cr ratio on the phase formation and corrosion behavior was investigated. By refining the grains, the addition of Co has an effect on both the microstructure and the corrosion. In addition, the ratio of aluminum to chrome has an effect on the microstructure as well as the behavior of corrosion. The synthesis of AlCoCrFeMnNi HEAs utilizing melting and casting as the process was the first step in this research project. The samples that were synthetically produced were analyzed using x-ray diffraction and optical microscopy respectively.

Keywords: High entropy alloys (HEAs), X-ray diffraction; Optical Microscopy, Corrosion behavior

1. Introduction:

Among all components of the alloy, aluminium shows the largest impact on the structure and properties; hence, the amount of information regarding AlxCoCrFeNi alloy. As the aluminium content of the AlxCoCrFeNi alloy increases, the fcc phase turns into the bcc phase [1,2]. For x in the molar ratio, the structure changes as follows: fcc occurs when x 0.4, a mixed fcc and bcc phase appears between 0.5 x 0.9, a single bcc phase is present when x 0.9 [3]. Through spinodal decomposition, the bcc phase consists of disordered bcc (A2) and ordered bcc (B2) [4]. Guo et al. indicate that the stability of the bcc or fcc in HEAs are associated with the concentration of valence electrons [5]. The change from fcc to bcc by increasing the Al content is also considered to occur due to lattice distortion. The alloys form a structure with lower atomic-packing efficiency, which is bcc due to the larger Al atomic size than the other major components [6].

Ogura et al. [7] explained the effect of Al content content on the phase transition. For this purpose, he used first principles electronic structure calculations. They claimed that the transformation from fcc to bcc with increasing Al content is mainly because of the high energy gain of the DO3 structure with Al addition. They observed that with increasing Al content, the total energy difference between fcc and bcc decreases. They pointed out that Cr and Fe stabilize the bcc structure, and Ni and Co are fcc stabilizers.

Other studies also indicate that there is significant elemental segregation in the dendritic and interdendritic regions in the AlxCrCoFeNi alloy. The dendritic regions are enriched in NiAl, while the interdendritic regions show an increased FeCr content [8]. For as-cast alloys, the microstructure also changes with the change in Al content [9]. The solidified microstructure changes from a columnar cellular when x in the molar ratio is up to 0.3 to a columnar dendritic structure when 0.4 x 0.6, then to equiaxed non-dendritic grain when 0.7 x 0.8, next to equiaxed dendritic grains when 0.9 x 1.5 and finally to non-equiaxed dendritic structures when 1.8 x 2.0 [57]. The Al content also affects other properties of the alloy. Increasing the aluminium content in the AlxCoCrFeNi alloy increases its strength while decreasing its plasticity [10].

All HEAs showed significantly higher wear resistance than AISI 304 at temperatures above 300 ◦C and Inconel 718 at temperatures greater than 800 ◦C. The study showed a positive effect of increasing Al content in AlxCoCrFeNi alloy on wear properties. The AlxCoCrFeNi alloy with a low aluminium content shows weak magnetic properties, while a high content makes the alloy ferromagnetic. This is due to the change in the crystal structure of the alloy from the fcc phase to the bcc phase [11]. Studies indicate that as the Al content in AlxCoCrFeNi alloy increases, the corrosion resistance decreases due to the porosity and inferior nature of the Al protection oxide film in these alloys [12].

2. Materials and Synthesis

2.1. Materials Al, Co, Cr, Fe, Mn, Ni powders were used to synthesize HEAs with different compositions. The composition for different HEAs is given in Table 1. The content of each element is shown in weight %. The HEAs are designated by H_1, $H_{0.33}$, H_1, H_3, and H_∞ according to their Al/Cr ratio. The Mn content has been taken in lesser amount because it deteriorates the corrosion performance in NaCl solution. The Ti has been added to HEAs as minor element because it helps in improving the corrosion resistance either by forming TiO_2 passive layer or by helping in the formation of other passive layers such as Cr_2O_3, Al_2O_3 etc.

Table 1 Composition of HEAs

Al	Co	Cr	Fe	Mn	Ni	Ti	Al/Cr ratio	Alloy
0	23	25	23	4	23	2	0	H_1
7	22	21	22	4	22	2	0.33	$H_{0.33}$
14	22	14	22	4	22	2	1	H_1
21	22	7	22	4	22	2	3	H_3
28	23.33	0	23.33	4	23.33	2	∞	H_∞

2.2. *Sample Preparation:* The powders as per the compositions were compacted using a uniaxial compaction apparatus after blending the powder. As a result, the green pellet with diameter 15 mm were formed by applying 90 MPa of pressure for 3 minutes. After 3 minutes, the pressure valve was opened and pressure was released. Then, the pellet was removed from the die carefully. Now, the compacted powder had strength enough to bear further synthesis processes

2.3. Melting and casting Process: Materials are melted by arc melting, which is commonly employed to create alloys. An electric arc is created by striking metals in a crucible in the copper hearth with a tungsten electrode. The chamber is emptied and subsequently refilled with argon gas in vacuum arc melting. As a result, melting takes place in an argon-free environment.

3. Results and Discussion

3.1. *Optical microscopy*

For H0 and H0.33 samples, the optical micrographs were almost same as shown in Figure 1. The samples revealed single phase multi-grained microstructure. The grain boundaries are clearly visible after etching the samples. The average grain size was estimated using imageJ software. The grain size was 54 microns for H0 and 41 microns for H0.33. It reveals that the increase of Al/Cr ratio refined the grain size due to which the grain size reduced from 54 to 41 microns.

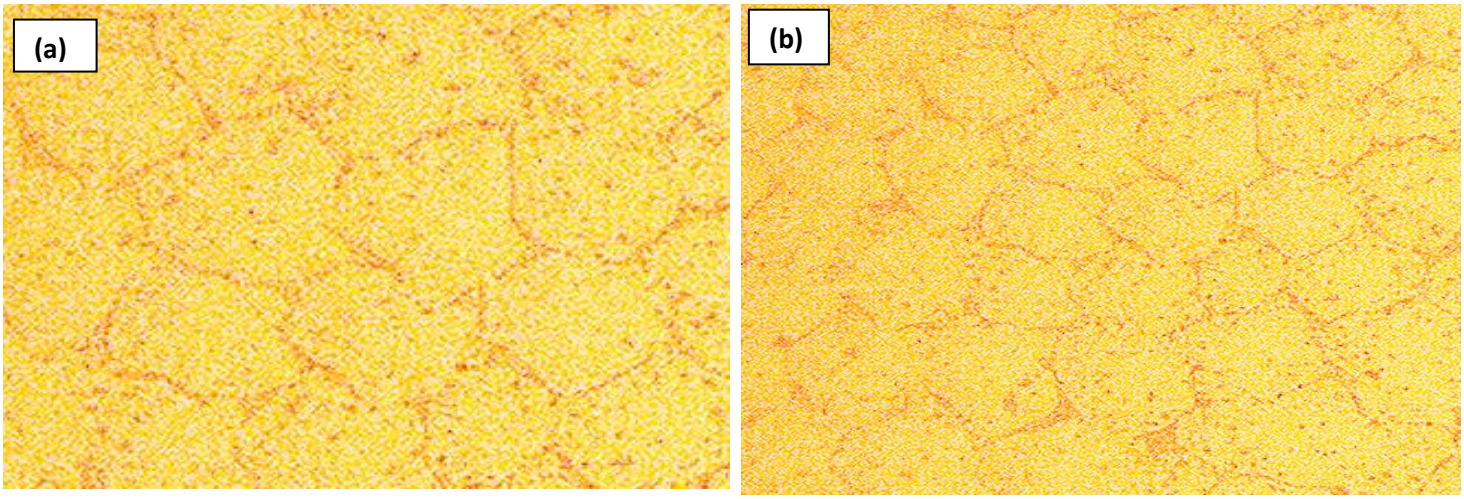

Figure 1 Optical micrograph for a) H_0 and b) $H_{0.33}$

The Al/Cr ratio was further increased from H0.33 to H∞ HEA. When the ratio increased to 1, the etchant samples showed two different phases in contrast as shown in Figure 2.The optical microscopy can show the number of phases by contrasting between them using etchant but it is not possible to identify that what phases are formed. To know about the phases, it is essential to go for X-ray diffraction. With further increase of Al/Cr ratio for H3 and H∞, the second phase increased its volume as shown in Figure 3.For H∞ HEA, phase I disappeared and only phase II seemed to be appeared all over the surface as shown in Figure 3 b.

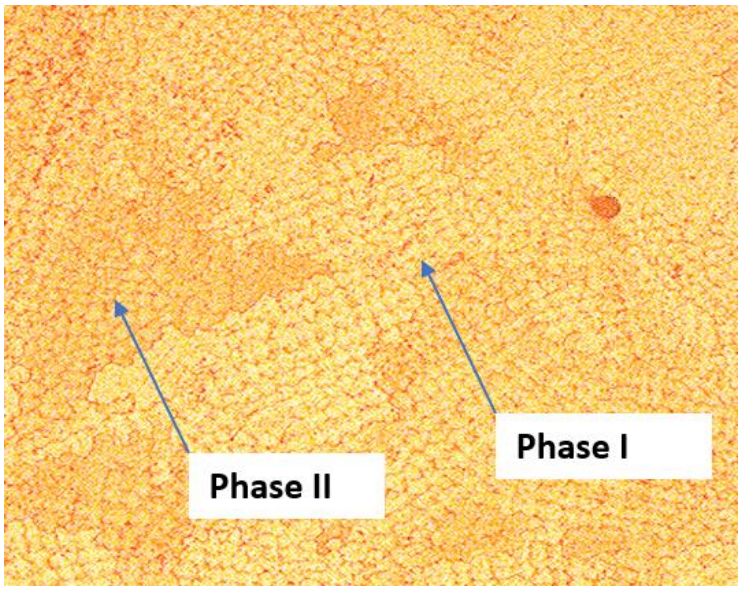

Figure. 2 Optical micrograph for H_1

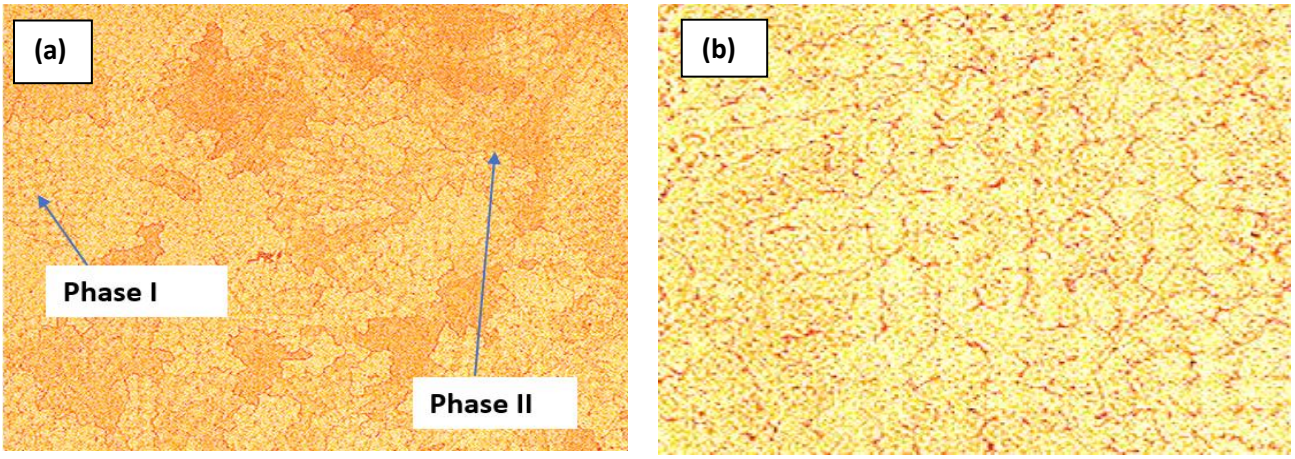

(a) **(b)**

Figure 3 Optical micrograph for a) H_3 and b) H_∞

3.2. X-Ray Diffraction (XRD)

Figure 4 a represents the XRD plot for H_0 HEA sample. Majority of FCC peaks are significant in the XRD plot. Three major FCC peaks are clearly visible in XRD graph, i.e., (111), (200), and (220). Similarly, $H_{0.33}$ HEA showed single FCC phase with prominent peak of (111). The diffracted planes that create the greatest intensities have the largest number of atoms with the highest number of electrons in the unit cell of the investigated materials, according to the XRD reflection with prominent peak intensity. It's also worth mentioning that simple phase zones may form in a multiprincipal alloy system, which defies the phase rule. With the exception of temperature, this finding means that the concentrations of the many components in these solid-solution phases may be changed within specific ranges while the single phases remain intact.

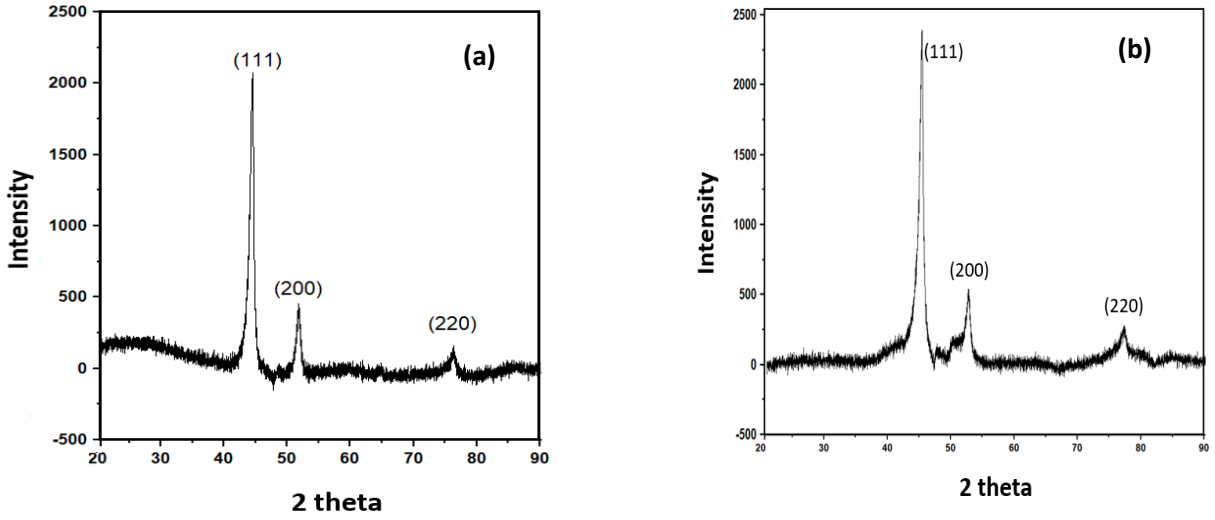

Figure 4 XRD plot for a) H_0 and b) $H_{0.33}$ HEA

Thee XRD Plots for the H_1 and H_3 samples are shown in Figure 5. The FCC phase sustained with three major peaks, i.e., (111), (200), and (220). However, some BCC peaks appeared along with the FCC phase. The appearance of BCC peaks could have contributed by increasing Al/Cr ratio, i.e., increasing Al content. It indicates that Al stabilizes the BCC phase due to which BCC peaks appeared with the increase of Al/Cr ratio. With further increase of Al/Cr ratio, only single phase was observed as seen in

the optical micrograph of H_∞. This single-phase would be BCC phase which means that higher Al/Cr ratio results in domination of BCC phase of FCC phase. There is a interesting effect of phases on corrosion behavior which is discussed in the next section.

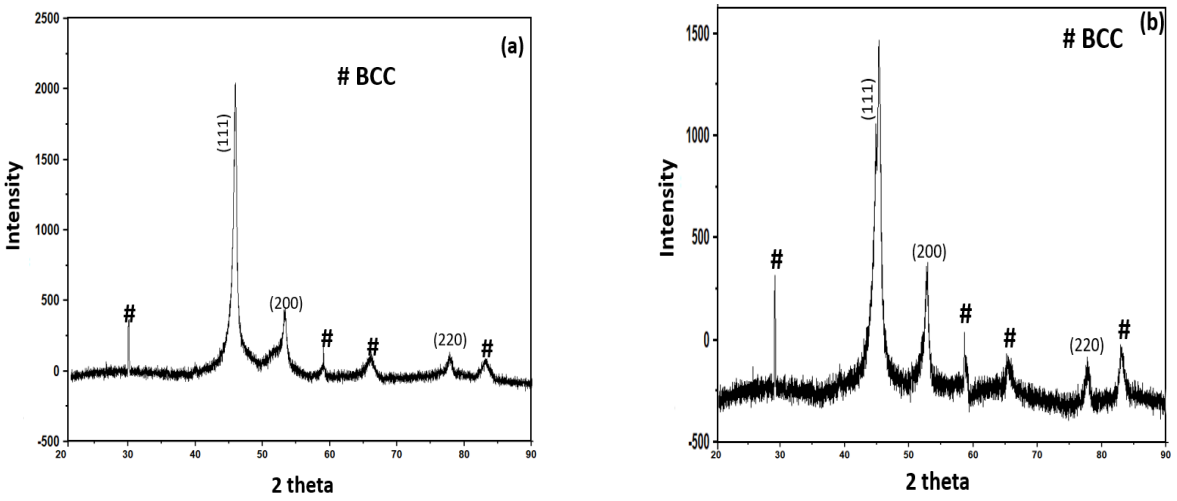

Figure 5 XRD plot for a) H_1 and b) H_3 HEA

4. Conclusion:

In the present study, the Al/Cr ratio was varied in HEAs and its effect was analyzed on microstructure, phase, hardness, and corrosion behavior. The main outcomes of the research work are stated as the H_0 and $H_{0.33}$ HEAs formed single FCC phase, confirmed using XRD analysis. H_1 and H_3 samples showed mixture of FCC and BCC phases.H_∞ sample showed single BCC phase. The hardness of HEAs increased with the increase of Al/Cr ratio due to high Al content which provided strengthening mechanism.

References:

1. Tong, C.-J.; Chen, Y.-L.; Yeh, J.-W.; Lin, S.-J.; Chen, S.-K.; Shun, T.-T.; Tsau, C.-H.; Chang, S.-Y. Microstructure Characterization of AlxCoCrCuFeNi High-Entropy Alloy System with Multiprincipal Elements. *Metall. Mater. Trans. A* **2005**, *36*, 881–893.

2. Kao, Y.-F.; Chen, T.-J.; Chen, S.-K.; Yeh, J.-W. Microstructure and Mechanical Property of As-Cast, -Homogenized, and -Deformed AlxCoCrFeNi (0≤x≤2) High-Entropy Alloys. *J. Alloys Compd.* **2009**, *488*, 57–64.

3. Wang, W.-R.; Wang, W.-L.; Wang, S.-C.; Tsai, Y.-C.; Lai, C.-H.; Yeh, J.-W. Effects of Al Addition on the Microstructure and Mechanical Property of AlxCoCrFeNi High-Entropy Alloys. *Intermetallics* **2012**, *26*, 44–51.

4. Praveen, S.; Kim, H.S. High-Entropy Alloys: Potential Candidates for High-Temperature Applications—An Overview. *Adv. Eng. Mater.* **2017**, *20*, 1700645.

5. Guo, S.; Ng, C.; Lu, J.; Liu, C.T. Effect of Valence Electron Concentration on Stability of Fcc or Bcc Phase in High Entropy Alloys. *J. Appl. Phys.* **2011**, *109*, 103505.

6. Wang, F.; Zhang, Y.; Chen, G. Atomic Packing Efficiency and Phase Transition in a High Entropy Alloy. *J. Alloys Compd.* **2009**, *478*, 321–324.

7. Ogura, M.; Fukushima, T.; Zeller, R.; Dederichs, P.H. Structure of the High-Entropy Alloy AlxCrFeCoNi: Fcc versus Bcc. *J. Alloys Compd.* **2017**, *715*, 454–459.

8. Manzoni, A.; Daoud, H.; Völkl, R.; Glatzel, U.; Wanderka, N. Phase Separation in Equiatomic AlCoCrFeNi High-Entropy Alloy. *Ultramicroscopy* **2013**, *132*, 212–215.

9. Geanta, V.; Voiculescu, I.; Milosan, I.; Istrate, B.; Mates, I.M. Chemical Composition Influence on Microhardness, Microstructure and Phase Morphology of AlxCrFeCoNi High Entropy Alloys. *Rev. Chim.* **2018**, *69*, 798–801.

10. Joseph, J.; Jarvis, T.; Wu, X.; Stanford, N.; Hodgson, P.; Fabijanic, D.M. Comparative Study of the Microstructures and Mechanical Properties of Direct Laser Fabricated and Arc-Melted AlxCoCrFeNi High Entropy Alloys. *Mater. Sci. Eng. A* **2015**, *633*, 184–193.

11. Kao, Y.-F.; Chen, S.-K.; Chen, T.-J.; Chu, P.-C.; Yeh, J.-W.; Lin, S.-J. Electrical, Magnetic, and Hall Properties of AlxCoCrFeNi High-Entropy Alloys. *J. Alloys Compd.* **2011**, *509*, 1607–1614.

12. Kao, Y.-F.; Lee, T.-D.; Chen, S.-K.; Chang, Y.-S. Electrochemical Passive Properties of AlxCoCrFeNi (X=0, 0.25, 0.50, 1.00) Alloys in Sulfuric Acids. *Corro. Sci.* **2010**, *52*, 1026–1034.